Stoichiometry of Anodic Copper Dissolution at High Current Densities

K. Kinoshita,*[1] D. Landolt,*[2] R. H. Muller,* and C. W. Tobias*

Inorganic Materials Research Division, Lawrence Radiation Laboratory and Department of Chemical Engineering, University of California, Berkeley, California 94720

ABSTRACT

The influence of current density, flow rate, and electrolyte composition on the stoichiometry of anodic copper dissolution was investigated under conditions comparable to those of electrochemical machining. Weight loss measurements, x-ray diffraction, and chemical analysis were used for the characterization of the dissolution reaction. A sharp change in dissolution mechanism coincided with the transition from active to transpassive dissolution. For active dissolution, an apparent valence of the dissolution process of two was found in sulfate and nitrate electrolytes, and of one in chloride electrolytes. For transpassive dissolution, mixed valences lying between 1 and 2 were found in all electrolytes. The mixed valences are interpreted to result from the simultaneous production of monovalent and divalent reaction products, some of which are in solid form.

Anodic dissolution of metals at current densities of up to several hundred amperes per square centimeter and with electrolyte flow velocities of many meters per second is being carried out on a technical scale in the process of electrochemical machining (ECM). In an attempt to provide quantitative information on the electrochemical processes under high current densities, the anodic dissolution of copper is being investigated (1-3). Copper was chosen because its electrochemical properties are reasonably well understood (4-8). In a previous paper (1), the role of mass transfer in determining the occurrence of passivation phenomena during copper dissolution in K_2SO_4 and KNO_3 solutions has been reported. It was found that apparent anode potentials and surface textures resulting from dissolution changed drastically while going from a low voltage (active) to a high voltage (transpassive) mode of dissolution.[3]

In the present study, the valence of the electrode reaction and the composition of reaction products of copper have been investigated in nitrate, sulfate, and chloride electrolytes. Weight loss measurements of the anode, x-ray diffraction analysis of solids, and chemical analysis of the solution were used for the characterization of the dissolution reaction. Current densities employed ranged from 0.1 to 80 A/cm^2. Experiments were performed under forced convection conditions in a flow channel at flow rates from 30-700 cm/sec, as well as in unstirred solutions under free convection conditions.

Experimental

Most experiments were carried out under forced convection conditions in an experimental flow system similar to that described in a previous study (1) and schematically shown in Fig. 1. The electrolyte was pumped by a positive displacement pump,[4] and the flow rate was measured with a rotameter.[5] One half inch stainless steel pipes were used throughout the system.

A 30 cm long rectangular flow channel of 1 x 3 mm cross section, constructed of laminated polyvinyl chloride, was positioned upstream of the experimental cell to establish fully developed velocity profiles at

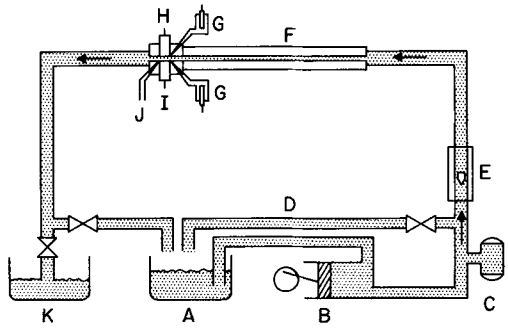

Fig. 1. Schematic of flow system: A, supply tank; B, dual piston pump; C, accumulator; D, bypass line; E, rotameter; F, entrance length of flow channel; G, reference electrodes; H, cathode; I, anode; J, capillary for precipitate collection; K, drain tank.

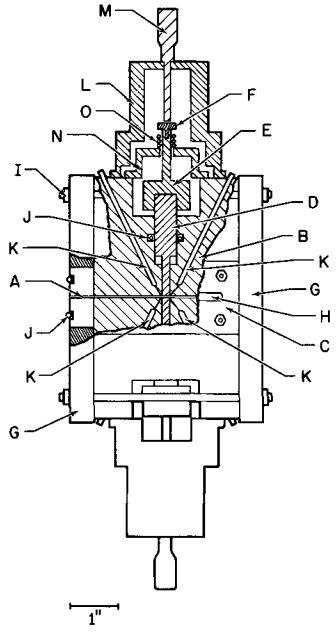

Fig. 2. Side view of experimental cell with partial cross sectioning: A, rectangular flow channel; B, epoxy cell body; C, stainless steel side plate; D, copper electrode; E, aluminum cap; F, nylon screw; G, stainless steel end flange; H, glass side window; I, bolt and nut assembly; J, O-ring seal; K, liquid junction connection to backside capillaries; L, aluminum micrometer holder; M, micrometer head; N, aluminum base plate; O, coil spring.

* Electrochemical Society Active Member.

[1] Present address: Pratt & Whitney Aircraft Corporation, Middletown, Connecticut 06457.

[2] Present address: University of California, School of Engineering & Applied Science, Los Angeles, California 90024.

Key words: anodic metal dissolution, copper anode, passivity.

[3] Different definitions for the phenomenon of passivation can be found in the literature. The term is used here to describe an abrupt increase in measured anode potential with time for certain combinations of flow rate and current density (see e.g., Fig. 3).

[4] Constametric Pumps, Milton Roy Company, Philadelphia, Pennsylvania. Varidrive Motor, U. S. Electrical Motors, Inc., Los Angeles, California.

[5] Type 18410, Schutte and Koerting Company, Cornwall Heights, Pennsylvania.

the electrodes (1). The electrolysis cell is shown schematically in Fig. 2. The cell body (B) was made of epoxy resin with the two glass side walls (H) held together by plates (C). The cell was connected to the inlet and outlet channel by end flanges (G). Optical observation of the interelectrode gap could be performed through the glass walls. Back-side capillaries (K) which enter the channel walls next to the electrodes were used for electrode potential measurements and, in some experiments, for the sampling of solution on the downstream side of the electrodes. The copper electrodes (D) (purity ≧99.9%) had a geometrical surface area of 3 x 3 mm. The electrodes could be advanced manually by turning micrometer head (M). The electrode assembly was pushed back against insert (F) by sprint (O). Silicone rubber gaskets[6] cast between glass wall and epoxy cell body were used for sealing the cell.

Measurements of cell voltage, electrode potentials, and current were made simultaneously on a multi channel light beam oscillograph.[7] Electrical power connections to the cell were made by threaded connections screwed into aluminum cap (E). The current was recorded by measuring the voltage drop across a shunt. Anode and cathode potentials were measured with respect to saturated calomel reference electrodes, which were placed in small glass containers connected to the capillaries by Tygon tubing. The electrolysis current was provided by an electronically controlled constant current supply.[8]

Prior to each run, the electrodes were ground on 600 grit emery paper and washed with aqueous detergent. Following a dip in concentrated HCl, they were rinsed with distilled water and reagent grade acetone and stored in vacuum until use. The electrodes were aligned with the channel wall by using a microscope with 20X magnification. During electrolysis, the 1 mm electrode gap was approximately maintained by manual adjustment of the micrometer.

During a typical experiment, 25 mg of copper were dissolved, which corresponded to an average depth of dissolution of about 0.3 mm. After each run, the anode was removed from the cell, rinsed with water, dried with acetone, and weighed on an analytical balance. The accuracy of the weight loss determination is estimated at ±1-2%. The amount of charge passed during the experiment was determined from the oscillographically recorded current trace. The accuracy of the charge measurement is estimated at ±2-3%.

From the measurement of charge and weight loss, an apparent valence n of the dissolution process was calculated according to Eq. [1]

$$n = \frac{ItM}{\Delta W \mathbf{F}} \qquad [1]$$

where I is the current passed during time t, M is the atomic weight of copper, ΔW is the anode weight-loss, and $\mathbf{F}$ is the Faraday constant.

Solid reaction products formed during the anodic dissolution of copper were analyzed by x-ray diffraction. Initial analyses were made using a 11.46 mm Debye-Scherrer powder camera mounted on an x-ray diffraction unit.[9] Ni filtered Cu radiation (40 kV, 20 mA) was used.

A sample of the anodic reaction product from the flow cell was collected by rubbing a glass fiber through the precipitate adhering to the wet surface. Diffraction patterns obtained were, however, difficult to analyze because of the faintness of the diffraction lines. Also, because of the small samples, exposure times to the x-ray beam from 6-12 hr were necessary.

[6] Encapsulant 502 RTV, Dow Corning Corporation, Midland, Michigan.
[7] Series 2300, Brush Instrument Division, Cleveland, Ohio.
[8] Type C618, Electronic Measurements Company, Eatontown, N. J. or Model KS 120-10M, Kepco Inc., Flushing, New York.
[9] Norelco X-Ray Diffraction Unit, Type 12045 with Debye-Scherrer Camera Type 52056-O, North American Philips Company, Inc., New York, N. Y.

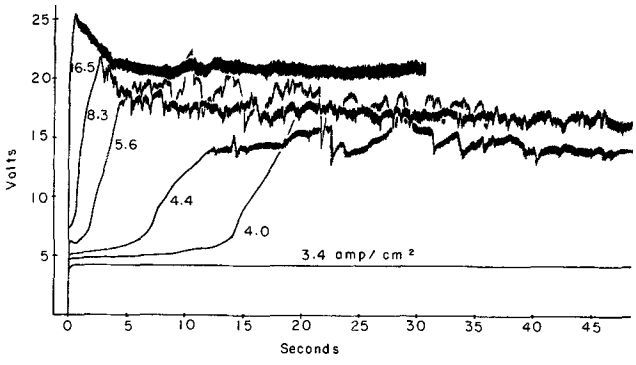

Fig. 3. Cell voltage transients measured in 2N KNO_3 at different current densities, flow rate 30 cm/sec.

To provide a larger specimen, a continuous sampling technique was developed. An x-ray diffractometer[10] using a Ni filtered Cu radiation (40 kV, 14 mA) could then be used. Solution escaping through the (0.014 in. diameter) capillary on the downstream side of the anode was collected on a Whatman No. 41 paper by continuous vacuum filtration. Without washing, the filter paper with adhering precipitate was dried under vacuum, mounted on a Lucite sample holder using double-sided adhesive tape, and placed in the diffractometer. A preliminary x-ray pattern of the blank showed strong diffraction peaks at low θ values which did, however, not interfere with the diffraction peaks of possible compounds present in the precipitate.

In order to substantiate the apparent valence determination carried out under forced convection conditions, some experiments were performed in a stagnant electrolyte which allowed quantitative determination of dissolved Cu^+ and Cu^{2+} ions. Since Cu^+ is unstable in aqueous solution unless complexing agents are present, only chloride electrolytes were analyzed this way. The electrolysis was carried out in an H cell with a glass frit separating anode and cathode compartments (2). In contrast to the highly diluted dissolution products obtained in the flow channel, concentrations which can be determined by simple analytical techniques could be obtained in this system. The analytical determination of Cu^{2+} and Cu^+ was based on that given by Vogel (9). Cuprous ion was oxidized with ferric ammonium sulfate, and the resulting ferrous ion was titrated with ceric sulfate. The cupric ion concentration was obtained as the difference between total copper concentration and cuprous ion concentration. The total copper concentration was determined iodometrically after oxidation of cuprous ion to cupric ion by sodium peroxide.

Results

Current-voltage behavior.—Figure 3 illustrates the transient cell voltage behavior during galvanostatic copper dissolution in 2N KNO_3 under a given flow rate (30 cm/sec). At low current density (3.4 A/cm²), the dissolution proceeds indefinitely in a low voltage (active) mode. Above a critical current density, which is shifted to higher values by increased flow rates, the dissolution process switches to a high voltage (transpassive) mode, after a transition time with active dissolution. The length of the transition period decreases with increasing current density and decreasing flow rate (not shown). Figures 4 and 5 are examples of transient cell voltage behavior with K_2SO_4 and KCl solutions. In all cases, dissolution in the transpassive mode occurs at a cell voltage which is 10-20V higher than in the active mode. Voltage fluctuations are observed in the transpassive region and, at the higher current densities, a voltage maximum occurs before steady state is reached.

Apparent valence.—Average steady-state values of the cell voltage and apparent valence values are

[10] Picker X-Ray Corporation, Waite Manufacturing Division, Inc., Cleveland, Ohio.

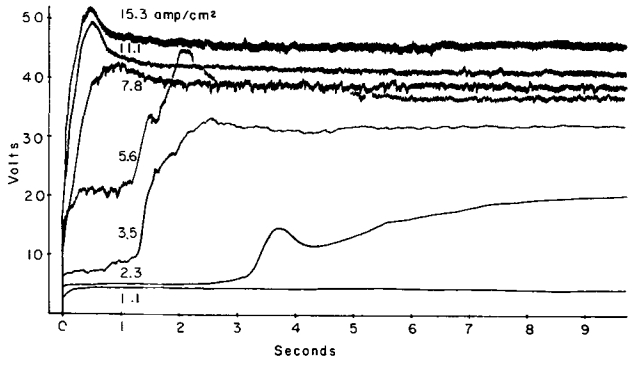

Fig. 4. Cell voltage transients measured in 1*N* K_2SO_4 at different current densities, flow rate 50 cm/sec.

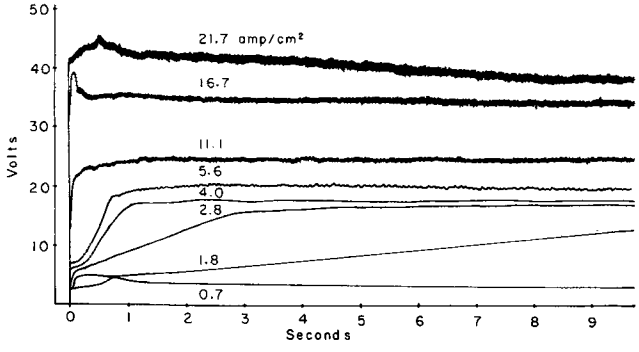

Fig. 5. Cell voltage transients measured in 2*N* KCl at different current densities, flow rate 50 cm/sec.

plotted *vs.* current density in Fig. 6 to 8. The behavior in 2*N* KNO_3 and 1*N* K_2SO_4 solutions is very similar. With the transition from active to transpassive dissolution, a sharp drop in apparent valence occurs. The apparent valence value of $n = 2$ observed in the active region indicates that copper is dissolved almost exclusively to divalent cupric ions. This is consistent with expectations based on thermodynamic considerations of the reversible potential of a copper electrode in contact with dissolved mono and divalent copper ions (8). In the transpassive region, on the other hand, the apparent valence depends on the value of the applied current density with respect to the current density at which passivation occurs. A limiting value of $n \simeq 1.5$-1.6 is reached at high current densities. In order to account for this value of n, it has to be assumed either that part of the copper is dissolved to a monovalent form, or that part of the metal disintegrates during the dissolution process. Since *p*H might have an influence in determining the reaction path (8), additional experiments were performed in a 2*N* KNO_3 solution adjusted to *p*H 1 by the addition of concentrated nitric acid, and also in a 1*N* H_2SO_4 solution. Voltage readings and apparent valences obtained in both of these electrolytes corresponded within experimental accuracy to those of the nitrate and sulfate solutions, respectively. This indicates that, within the range studied, *p*H has a negligible influence on apparent valence of the dissolution process. As illustrated by Fig. 8, the behavior in KCl solutions was quite different from that in KNO_3 and K_2SO_4 solutions. A sharp transition between active and transpassive dissolution was absent. Instead, periodic fluctuations occurred (indicated by dotted lines in Fig. 8) in the transition region. Such oscillations in the copper/chloride system have also been reported in the literature for low current density conditions (6, 10). Periodic oscillations have also been observed during high rate copper dissolution in sulfate and chlorate electrolytes under certain conditions (1-3). The apparent valence, in the case of chloride solution, is $n = 1$ at low current densities. A maximum of $n = 1.4$ is observed at intermediate current densities, and the apparent valence drops to $n \simeq 1.2$ in the range of high current densities. While it appears that the observed changes in apparent valence are related to the occurrence of passivation, the relationships are not as clear cut as in

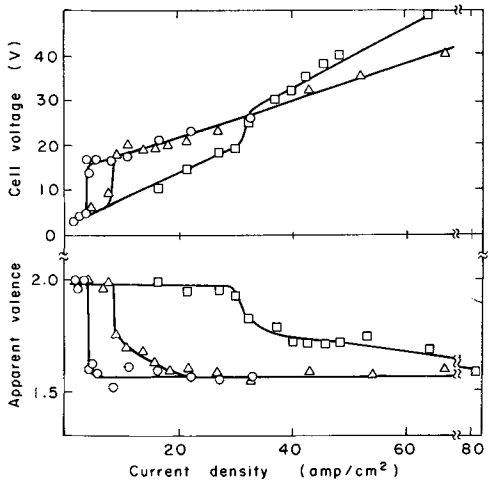

Fig. 6. Variation of apparent valence and cell voltage with current density in 2*N* KNO_3 for different flow rates: ○, 30 cm/sec; △, 200 cm/sec; □, 627 cm/sec.

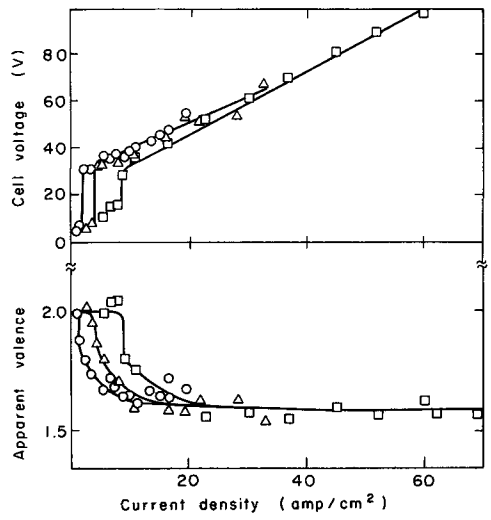

Fig. 7. Variation of apparent valence and cell voltage with current density in 1*N* K_2SO_4 for different flow rates: ○, 50 cm/sec; △, 200 cm/sec; □, 686 cm/sec.

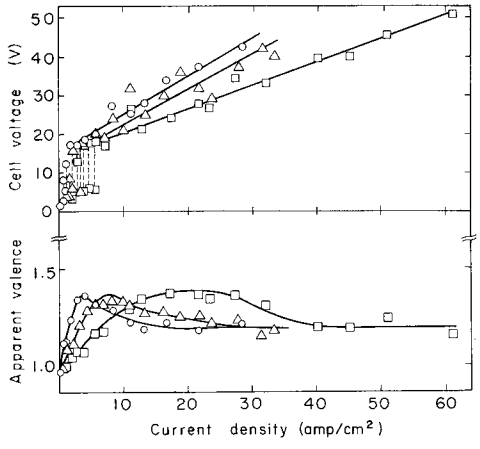

Fig. 8. Variation of apparent valence and cell voltage with current density in 2*N* KCl for different flow rates: ○, 50 cm/sec; △, 200 cm/sec; □, 606 cm/sec.

Table I. X-ray analysis of anode solid reaction products

Electrolyte	Compounds identified
2*N* KNO_3	Cu_2O, Cu
2*N* KNO_3 + HNO_3 (pH 1)	Cu
1*N* K_2SO_4	Cu_2O, Cu
1*N* H_2SO_4	Cu

nitrate and sulfate solutions. For example, at the highest flow rate (606 cm/sec), the maximum value of n was attained at much higher current density than that corresponding to the active-passive transition derived from cell voltage measurements.

Analysis of solid reaction products.—Anode precipitates were found during transpassive dissolution only. X-ray analysis of precipitates collected from experiments performed in KNO_3 and K_2SO_4 solutions showed Cu_2O to be the principal copper compound. Diffraction peaks for metallic copper were also present in some experiments. The metallic copper contents of precipitates from acidified solutions was increased at the expense of the cuprous oxide contents (Table I). No analysis of anodic precipitates in chloride solution was possible because precipitates could not be collected in sufficient amounts. A typical diffraction pattern of anode precipitate is given in Fig. 9 together with patterns of known samples of Cu_2O and Cu. Precipitates collected in the drain tank showed a different composition from those collected close to the anode. They contained basic oxides of complex composition, owing to contact with the alkaline solution produced at the cathode.

Analysis of dissolved reaction products.— Apparent valence determinations in chloride solution were also carried out in a separate cell under absence of forced convection. In these experiments, values of apparent valence obtained from weight loss measurements could be compared with those obtained by chemical analysis of dissolved reaction products. Calculation of the chemically determined apparent valence n^* was based on Eq. [2]

$$Cu \rightarrow xCu^+ + yCu^{2+} + n^*e \qquad [2]$$

where x and y are the fractional amounts of Cu^+ or Cu^{2+}, respectively. Since, from the mass balance $x + y = 1$ and from the charge balance $x + 2y = n^*$, one gets Eq. [3]

$$n^* = 2 - x = 1 + y \qquad [3]$$

The results given in Table II illustrate the good agreement between the valence determined by chemical analysis with that derived from weight loss measurements for a wide range of current densities. In all cases a mass balance could be established within 1-2%. Changes in apparent valence with current density in chloride solutions are therefore indeed due to different ratios of Cu^+ and Cu^{2+} produced. No oxygen evolution was observed during the experiments. The experiments also confirmed that the anodic behavior, *i.e.*, the occurrence of active and transpassive dissolution, was essentially the same in stagnant as in flowing solutions,

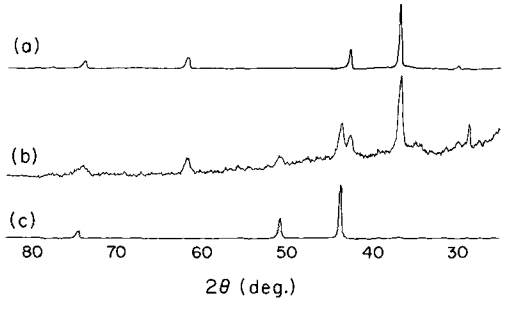

Fig. 9. X-ray diffractometer trace of anode precipitate (b) compared to known samples of Cu_2O (a) and Cu (c). Anode precipitate obtained at 11.1 A/cm² and 50 cm/sec in 1*N* K_2SO_4.

Table II. Chemical analysis of dissolved reaction products in 3*N* KCl solution after passage of 60 coul, anode area 1 cm²

Current density, A/cm²	Valence from dissolved Cu^+ and Cu^{++}	Valence from weight loss
0.05	1.00	1.00
0.10	1.19	1.15
0.13	1.21	1.28
0.16	1.27	1.31
0.21	1.28	1.30
0.26	1.26	1.28
0.51	1.22	1.20
0.82	1.19	1.20
1.00	1.13	1.10
1.31	1.14	1.16
1.58	1.10	1.08
1.87	1.08	1.06
1.98	1.07	1.07

with the exception that passivation sets in at much lower current densities in the absence of external convection.

Discussion

Nitrate and sulfate solutions.—Two dissolution modes, active and transpassive, were found differing in overvoltage and apparent valence of dissolution. The transition between active and transpassive dissolution depends on mass transfer conditions. Using the mass transfer correlations for channel flow discussed earlier (1), the interfacial concentration of ionic dissolution product at the onset of transpassive dissolution was estimated from the passivation current density for different flow rates and electrolytes. (A diffusion coefficient of 5×10^{-6} cm²/sec was assumed for this calculation.) A comparison of the results shown in Table III with solubility data given in Table IV indicates that the onset of transpassive dissolution coincides, at least qualitatively, with the limiting transport of dissolved reaction products by convective diffusion. This substantiates the validity of previous results (1) which were obtained in a different flow system, mostly at higher current densities and flow rates. In addition, it was found here that passivation current densities in 1*N* H_2SO_4 were essentially the same as in 1*N* K_2SO_4. This suggests that limitations in the transport of cupric salt, rather than the formation of oxide or hydroxide, initiates the change to transpassive dissolution.

The present study also demonstrates that the transition between active and transpassive dissolution is associated with a drastic change in current efficiency for the metal removal process, with more copper being

Table III. Calculated interfacial concentration of copper salts at onset of transpassive dissolution

Electrolyte	Flow velocity, cm/sec	Reynolds number	Passivation current density, A/cm²	Interfac. conc., moles/l
2*N* KNO_3	30	510	3.8	4.5
	200	3390	8.5	4.6
	627	10600	31.0	8.5
1*N* K_2SO_4	50	730	1.5	1.4
	200	2920	4.1	2.2
	686	10000	8.5	2.2
1*N* H_2SO_4	50	770	3.6	3.4
	200	3090	4.7	2.5
	686	10600	11.8	3.0
2*N* KCl	50	820	0.4	0.8
	200	3270	1.2	1.2
	606	10000	2.5	1.2

Table IV. Solubilities of copper salts at room temperature

Salt	Solvent	Solubility, moles/l	Reference
Cupric nitrate	H_2O	7.0	(24)
Cupric sulfate	H_2O	1.4	(24)
	1*N* H_2SO_4	1.1	(25)
Cuprous chloride	2*N* KCl	1.0	(17), (18)
	3*N* KCl	1.9	(17), (18)

dissolved for a given amount of charge in the transpassive region. A mechanism involving the formation of monovalent copper species at the anode, especially cuprous oxide, rather than anodic disintegration by grain boundary attack (11, 12), seems to be the cause for the apparent increase in current efficiency. The above conclusion, although it cannot be rigidly proven on the grounds of our results, is supported by the following experimental observations: (*A*) Cuprous oxide has been found to be the main constituent of anodic films. (*B*) Substantial amounts of metallic copper were observed in the x-ray patterns in acidic solutions only, consistent with the fact that Cu_2O disproportionates in these solutions into Cu^{2+} and Cu. (*C*) No grain boundary attack was observed microscopically in the transpassive region. Instead, the surfaces after transpassive dissolution had a shiny appearance and were almost randomly pitted (1, 2). (*D*) At least in the case of chloride solutions, the presence of cuprous ion could be verified quantitatively. All these factors indicate that a distintegration mechanism, which has been proposed primarily for more reactive metals (beryllium, magnesium, cadmium, zinc) at low current densities (13-16), is not likely to be of importance in the present anodic dissolution process.

Measured apparent valences tended to reach a constant limiting value at high current densities. No satisfactory explanation for this phenomenon can be given at the present time. From a purely kinetic point of view we would expect a continuous variation of n with current density. A possible explanation of the observed constancy of n may, perhaps, be sought in a model viewing the surface as an ensemble of small surface area elements randomly fluctuating between active and passive states. Such active-passive fluctuations, which are most pronounced in chlorate electrolytes (2, 3), are now being studied in this laboratory.

Chloride solutions.—The dissolution behavior in chloride electrolytes is different because the monovalent ionic state becomes thermodynamically more favorable than the divalent state due to the formation of cuprous ion complexes (17, 18). Thus, disproportionation of Cu^+, which usually occurs in aqueous solutions is avoided. Since a variety of different complexes may be formed, depending on the local chloride concentration, the dissolution process in chloride solutions is expected to be much more complicated than in nitrate and sulfate solutions. For example, due to the effect of chloride concentration on the solubility of cuprous ion, the formation of precipitate layers depends not only on the rate of departure of cations from the interface, but also on the rate of arrival of anions. In addition to the mass transport of the dissolution product, the mass transport of chloride ion may therefore become a limiting factor, since chloride ions are consumed at the anode by complex formation. Such a mechanism has, for example, been reported by Landsberg *et al.* (19) for the dissolution of gold in HCl. During the course of stoichiometric determinations in stagnant solution, a number of transient measurements were performed in 3*N* KCl solutions at constant current density. Table V summarizes the transition times determined for the onset of transpassive behavior. In spite of that the geometrical arrangement was not ideal to exclude free convection completely, the application of Sand's equation is justified because of the short times involved. From the average measured quantity $i\sqrt{\tau}$, a value for ΔC, the rate-limiting concentration difference, was calculated according to Eq. [4]

Table V. Transition times τ for copper dissolution at different current densities i in 3*N* KCl without external convection

i, A/cm²	τ, sec	$i\sqrt{\tau}$
0.10	38.90	0.62
0.16	11.60	0.56
0.21	9.20	0.69
0.26	5.63	0.62
0.51	1.85	0.70
0.82	0.65	0.68
1.00	0.48	0.69
1.31	0.28	0.69
1.58	0.20	0.70
1.87	0.16	0.75
1.98	0.15	0.77

$$\Delta C = \frac{2i\sqrt{\tau}}{n\mathbf{F}\sqrt{\pi D}} \qquad [4]$$

assuming $D = 5 \times 10^{-6}$ cm²/sec and $n = 1$. The resulting value of $\Delta C = 3.6$ mole/liter is similar in magnitude to the solubility of CuCl in 3*N* KCl [1.9 mole/liter (17)]. This indicates that, under the conditions of these experiments, passivation may have been caused by a similar precipitation mechanism as in nitrate and sulfate solutions.

The increase in apparent valence n on passivation (Fig. 8) is consistent with the fact that at higher anode potentials, the reaction $Cu \rightarrow Cu^{2+}$ becomes thermodynamically possible. No true anode potential measurements were possible under the conditions of this study; therefore, a discussion has to remain qualitative. The subsequent decrease in n at still higher current densities may then be explained by assuming formation of Cu_2O, as observed in the case of nitrate and sulfate solutions. The oozing of a reddish brown, finely dispersed dissolution product from localized anode areas which changed their positions during electrolysis was observed visually in stagnant KCl solutions in the transpassive region (2). This solid might have been Cu_2O, but it was not possible to collect the precipitate due to its chemical instability in the chloride electrolyte. The formation of cuprous oxide during copper dissolution in chloride media has also been reported in the literature (20-23). The formation of a thin cuprous chloride film during transpassive dissolution in chloride solution was indicated by the white appearance of the surface.

Summary and Conclusions

1. The present study has confirmed earlier findings (1) obtained under different experimental conditions that in nitrate and sulfate electrolytes the transition from active to transpassive dissolution of copper is controlled by the mass transfer of dissolved dissolution products.

2. Although the details of copper dissolution in chloride solution are probably different from those in nitrate and sulfate, the gross current-voltage behavior is similar. Ionic mass transfer limitations seem, therefore, to be the dominating factor determining the onset of passivation in chloride solutions, too.

3. The apparent valence of the dissolution process undergoes a noticeable change with the transition from active to transpassive dissolution. In nitrate and sulfate solutions, active dissolution proceeds with an apparent valence of 2. Transpassive dissolution leads to a lower apparent valence, which reaches a limiting value of 1.6 at high current densities. This drop in apparent valence is interpreted to be caused by the anodic production of monovalent copper species, rather than by anodic disintegration.

4. Active dissolution in chloride solution occurs with an apparent valence of one. This is due to the stabilization of cuprous ion by complex formation. Upon passivation the apparent valence increases, going through a maximum of 1.4 with increasing current density before reaching a limiting value of 1.2. This increase in apparent valence on passivation is due to part of the copper being dissolved in divalent form.

5. No significant oxygen evolution occurred during copper dissolution under all the experimental conditions employed.

6. The formation of solid anodic dissolution products during transpassive dissolution has been demonstrated in agreement with earlier optical observations. Anal-

ysis of the precipitates by x-ray diffraction has shown Cu_2O to be the main constituent produced in potassium nitrate and sulfate solutions. Metallic copper, resulting from disproportionation of Cu_2O, is found in acidified solutions. In chloride solutions optical observation indicated the formation of cuprous chloride films.

Acknowledgment

This work was done under the auspices of the U. S. Atomic Energy Commission.

Manuscript received May 13, 1970.

Any discussion of this paper will appear in a Discussion Section to be published in the June 1971 JOURNAL.

REFERENCES

1. D. Landolt, R. H. Muller, and C. W. Tobias, *This Journal*, **116**, 1384 (1969).
2. K. Kinoshita, Ph.D. Thesis, University of California, Berkeley, UCRL-19051, Sept. 1969.
3. D. Landolt, R. Acosta, R. H. Muller, and C. W. Tobias, *This Journal*, **117**, 839 (1970).
4. E. Mattson and J. O'M. Bockris, *Trans. Faraday Soc.*, **55**, 1586 (1959).
5. A. Hickling and D. Taylor, *ibid.*, **44**, 262 (1948).
6. R. S. Cooper and J. H. Bartlett, *This Journal*, **105**, 109 (1958).
7. F. H. Giles and J. H. Bartlett, *ibid.*, **108**, 266 (1961).
8. M. Pourbaix, "Atlas of Electrochemical Equilibria in Aqueous Solutions," p. 384, Pergamon Press, New York (1966).
9. A. I. Vogel, "A Textbook of Quantitative Inorganic Analysis Including Elementary Instrumental Analysis," 3rd ed., John Wiley & Sons, Inc., New York (1961).
10. H. Lal and H. R. Thirsk, *J. Chem. Soc.*, **1953**, 2638.
11. U. R. Evans, "Corrosion and Oxidation of Metals," Arnold, London (1960).
12. I. A. Menzies and A. F. Averill, *Electrochim. Acta*, **13**, 807 (1968).
13. M. E. Straumanis and Y. Wang, *Corrosion*, **22**, 132 (1966).
14. M. E. Straumanis, J. L. Reed, and W. J. James, *This Journal*, **114**, 885 (1967).
15. M. E. Straumanis and B. K. Bhatia, *ibid.*, **110**, 357 (1963).
16. W. J. James, M. E. Straumanis, and J. W. Johnson, *Corrosion*, **23**, 15 (1967).
17. W. U. Malik, S. M. F. Rahman, and S. A. Ali, *Z. anorg. u. allgem. Chem.*, **299**, 322 (1959).
18. W. U. Malik, S. M. F. Rahman, and S. A. Ali, *ibid.*, **301**, 220 (1959).
19. G. Just and R. Landsberg, *Electrochim. Acta*, **9**, 817 (1964).
20. R. S. Cooper, *This Journal*, **103**, 307 (1956).
21. D. Miller, *J. Phys. Chem.*, **13**, 256 (1909).
22. H. W. Gillett, *ibid.*, **13**, 332 (1909).
23. A. G. Arend, *Paint Tech.*, **13**, 265 (1948).
24. Int. Crit. Tables **4**, 222, McGraw-Hill (1928).
25. W. J. Muller and L. Holleck, *Monatsh. Chem.*, **52**, 409 (1929).

Comparative Activity of (111), (100), (110), and Polycrystalline Platinum Electrodes in H_2-Saturated 1M H_2SO_4 under Potentiostatic Control

Sigmund Schuldiner,* Murray Rosen,*[1] and David R. Flinn*[1]

Electrochemistry Branch, Naval Research Laboratory, Washington, D. C. 20390

ABSTRACT

Potentiostatic measurements of the three principle faces of oriented single Pt crystals and polycrystalline Pt showed some interesting comparisons. True areas are based on Pt atom densities, and under the electrochemical treatment used, no changes in these areas were found once the initial surface cleaning was completed. The hydrogen overvoltage was independent of crystal orientation or other metallurgical factors; however, the passivation of the hydrogen oxidation reaction and the oxygen generation reactions were different for each single crystal orientation with a large difference between these faces and a polycrystalline bead electrode. Steady-state relations between potential and amounts of associated H atoms and number of sites available for coverage with O atoms were determined also. These steady-state values are generally less than the comparative amounts found under transient conditions. Oxygen evolution on the Pt faces was not observed below a potential of 1.8V. It appears that grain boundaries, stress, and impurity inclusions may have more effect in determining the catalytic activity for some reactions than does the actual atomic density or geometry of Pt atoms.

Although there have been numerous investigations of the hydrogen reaction on polycrystalline Pt electrodes and of the potentiostatic behavior of Pt in H_2-saturated solutions, our knowledge of the effects of the geometry of Pt atoms on such behavior is very limited. Using the voltage sweep method, Will (1) studied the relationship between hydrogen adsorption and potential on single Pt crystals of (111), (100), and (110) orientations.

Our approach was to conduct a comparative investigation of polycrystalline Pt with Pt single crystal orientations with respect to reactivity for steady-state hydrogen generation, hydrogen oxidation, and oxygen generation reactions. In addition, steady-state relations between surface coverage with potential were determined, both in the presence and absence of dermasorbed oxygen.

Experimental

The high-purity, gas-tight electrochemical system, the experimental conditions, and the method of measurement were the same as used in ref. (2). Three single crystal Pt electrodes with orientations (111), (100), and (110) were in the cell. A fourth Pt electrode, polycrystalline bead, similar to previous ones (2), was substituted for one of the single crystal electrodes to confirm that the experimental conditions

* Electrochemical Society Active Member.
[1] National Academy of Sciences-National Research Council Postdoctoral Research Associates at NRL.
Key words: overvoltage, adsorption, catalysis, atom geometry, dermasorption.